

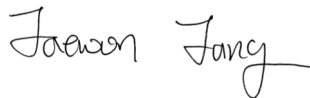
Oil & Natural Gas Technology

DOE Award No.: DE-FE0009927

Quarterly Research Performance Progress Report (October - December 2013)

Verification of capillary pressure functions and relative permeability equations for gas production

Submitted by:
Jaewon Jang



Wayne State University
DUNS #: 001962224
5050 Anthony Wayne Dr.
Detroit, MI 48202
e-mail: jaewon.jang@wayne.edu
Phone number: (313) 577-3854

Prepared for:
United States Department of Energy
National Energy Technology Laboratory

January 31, 2014



Office of Fossil Energy

SUMMARY

- Task 1.0 Project Management and Planning
Done
- Task 2.0 Pore Network Generation
Done
- Subtask 2.1 Information of relevant information of in-situ hydrate-bearing sediments
Done
- Subtask 2.2 Generation of sediment packing using Discrete Element Model (DEM)
Done
- Subtask 2.3 Extraction of pore-network from sediment packing
Done
- Task 3.0 Algorithm for conductivity and hydrate dissociation
Done
- Task 4.0 Characteristic Curve and Relative Permeability
In progress

Project timeline

	Year 1				Year 2				Year 3	
	Qtr1	Qtr2	Qtr3	Qtr4	Qtr1	Qtr2	Qtr3	Qtr4	Qtr1	Qtr2
Task 1.0 Project Management and Planning	[Solid black bar]									
Task 2.0 Pore Network Generation	[Solid black bar]									
Subtask 2.1: Information of grain size distribution	[Grey bar]									
Subtask 2.2: Sediment packing by DEM simulation	[Grey bar]									
Subtask 2.3: Extraction of pore network	[Grey bar]									
<i>Milestone A</i>	[Diamond marker]									
Task 3.0 Algorithm for conductivity and hydrate dissociation	[Solid black bar]									
<i>Decision Point 1</i>	[Circle marker]									
<i>Milestone B</i>	[Diamond marker]									
Task 4.0 Characteristic Curve and Relative Permeability	[Solid black bar]									
Subtask 4.1: Effect of network size/boundary condition	[Grey bar]									
Subtask 4.2: Effect of hydrate habit	[Grey bar]									
Subtask 4.3: Effect of hydrate saturation	[Grey bar]									
Subtask 4.4: Effect of gas viscosity	[Grey bar]									
Subtask 4.5: Effect of grain size distribution	[Grey bar]									
Subtask 4.6: Suggestion of fitting parameters	[Grey bar]									
<i>Decision Point 2</i>	[Circle marker]									
<i>Milestone C</i>	[Diamond marker]									

1. Introduction

Numerical simulation studies predict the long-term behavior of hydrate-bearing sediments during gas production [Kurihara et al., 2008; Moridis et al., 2009; Moridis and Regan, 2007a, 2007b; Anderson et al., 2011, Myshakin et al., 2011, 2012]. Numerical simulators for gas hydrate studies adopt many equations for coupled-process analysis. One of important equations is a relative permeability equation because it affects gas and water production rate and gas recovery efficiency during gas hydrate development [Johnson et al., 2011; Minagawa et al., 2004; Mingawaga et al., 2007; Kleinberg et al., 2003; Gupta, 2007; Jang and Santamarina, 2011, 2014]. Expressions for relative water k_{rw} and gas permeability k_{rg} as a function of water saturation S_w require appropriate fitting parameters [Corey, 1954; Brooks and Corey, 1964; Stone, 1970; van Genuchten, 1980; Parker et al., 1987; Anderson et al., 2011; Moridis et al., 2008]. Therefore, the selection of proper parameters for relative permeability equations is critically important to enhance the ability of hydrate simulators for predicting gas and water production rate. However, laboratory data or numerical simulation studies are not available to guide the selection of adequate fitting parameters for relative permeability equations.

The purpose of this paper is to suggest reliable fitting parameters for relative permeability equations by simulating gas expansion and calculating relative permeability using a pore-network model. Two types of relative permeability equations are introduced and the fitting parameters used in hydrate study are summarized in the following section.

2. Relative Permeability Equations for Gas Hydrate Production

The relative permeability of water k_{rw} (or gas k_{rg}) is the water (or gas) conductivity at a given water saturation S_w normalized by the water (or gas) conductivity at 100% water saturation (or gas). The conductivity at the irreducible phase saturation may be used as a reference value [Jaiswal, 2004]. In this study, water conductivity at 100% water saturation and gas conductivity at residual water saturation are used as reference values. Relative permeability varies as a function of saturation, and predictive models are intimately related to the water characteristic curve models [Fredlund and Xing, 1994; Fredlund, 2002].

Two popular types of relative permeability models follow .

$$k_{rw} = \bar{S}^{0.5} \left[1 - (1 - \bar{S}^{1/m})^m \right]^2 \quad (1)$$

van Genuchten-type

$$k_{rg} = (1 - \bar{S})^{0.5} \left[1 - \bar{S}^{1/m} \right]^{2m} \quad (2)$$

$$k_{rw} = \left(\frac{S_w - S_{rw}}{1 - S_{rw}} \right)^{n_w} \quad (3)$$

modified Stone-type

$$k_{rg} = \left(\frac{S_g - S_{rg}}{1 - S_{rw}} \right)^{n_g} \quad (4)$$

where S_{rw} is the residual water saturation, S_{rg} is the residual gas saturation, $\bar{S} = (S_w - S_{rw}) / (1 - S_{rw})$ is the relative water saturation [van Genuchten, 1980; Parker et al., 1987; Stone, 1970; Moridis et al., 2008]. The fitting parameters such as m -value for Equation 1 and 2, and n_w - and n_g -value for Equations 3 and 4 are needed for relative permeability calculation. The residual water S_{rw} and gas saturation S_{rg} need to be determined as well.

Relative water and gas permeability curves obtained by using several fitting parameters are shown in Figure 1. The van Genuchten-type equations shows that as the fitting parameter increases from $m=0.45$ to 1.1 , relative water permeability k_{rw} increases while relative gas permeability k_{rg} decreases at a given water saturation (Figure 1a). However, for modified Stone-type equations, as the fitting parameters n_w and n_g increase, both relative water and gas permeabilities decrease at a given water saturation (Figure 1b). The water permeability calculated using $m=0.9$ and gas permeability calculated using $m=1.1$ of van Genuchten-type equation are almost identical to the modified Stone-type water and gas permeability curves obtained with fitting parameters $n_w=n_g=3$.

The m -values obtained by conventional laboratory experiments that do not consider gas hydrate are compiled in Wösten et al. (1999). The m -values for 5521 European soil samples range from $m=0.0793$ for very fine-grained soils to $m=0.3424$ for coarse-grained soils. In the experiments performed in those conventional studies, water and gas invade from one boundary to the other boundary of a soil specimen [ASTM D6836]. However, gas nucleates at pores inside sediments during hydrate dissociation. This different gas generation mechanism may result in different gas permeability during gas invasion and gas nucleation [Yortsos et al., 1989; Poulsen et al., 2001].

Fitting parameters and residual water and gas saturation for relative permeability equations used in hydrate-bearing reservoir simulations are compiled by Jang and Santamarina (2014): $m \approx 0.45$, $S_{rw}=0.2 \sim 0.3$, and $S_{rg}=0.05$ for van Genuchten-type equation, $n_w=3.0 \sim 4.5$, $n_g=2.0 \sim 4.0$, $S_{rw}=0.1 \sim 0.25$, and $S_{rg}=0 \sim 0.02$ for modified Stone-type equation [Hong and Pooladi-Davish, 2003, 2005a, 2005b; Uddin et al., 2008; Moridis and Regan, 2007a, 2007b; Moridis and Sloan, 2007; Moridis et al., 2007, 2009; Reagan et al., 2010; Reagan and Moridis, 2008; Rutqvist and Moridis, 2007, 2009; Moridis and Kowalsky, 2005; Anderson et al., 2011; Kurihara et al., 2011; Gupta, 2007; Konno et al., 2010]. However, up to the authors' best knowledge, any supporting experiment or numerical study to validate these selected fitting parameters for hydrate simulation studies is not available in the literature.

In this paper, in order to suggest appropriate fitting parameters of relative permeability equations for gas production from hydrate-bearing sediments, a pore network model is developed to simulate gas expansion and calculate relative permeability.

3. Numerical Method and Procedure

A pore network model consists of pores connected by tubes. The method of pore network model generation, gas expansion, and permeability calculation is explained in this section.

Pore network model generation. Using the grain size distribution and the effective stress of in-situ hydrate-bearing sediments, a three-dimensional particle packing is generated by Discrete Element Modeling DEM (*Itasca, PFC 3D*). The grain size distribution of Mallik-Mackenzie Delta sandy sediments is selected for an input of DEM simulation [Soga et al., 2007; Jenner et al., 1999]. More information about grain size distribution of in-situ hydrate-bearing sediments can be found in Soga et al. (2007), Jenner et al. (1999), Ginsberg et al. (2000), and Tan (2004). After particles are generated, a confining pressure $\sigma'=5\text{MPa}$ equivalent to the effective stress of in-situ hydrate-bearing sediments at $\sim 500\text{m}$ below sea floor is applied to consolidate the particle packing (Figure 2a). Once the particle packing is obtained, the pore space of the packing is

extracted (Figure 2b). Then, the maximal ball algorithm developed by Silin and Patzek (2006), Al-Kharusi and Blunt (2007), Dong (2007), and Dong and Blunt (2009) is applied to extract three-dimensional pore network model (Figure 2c).

Hydrate distribution. Hydrates are randomly disseminated in pores to satisfy a target initial hydrate saturation. In numerical simulation, pores are fully filled with either hydrate or water because of Oswald ripening.

Gas expansion. Hydrates dissociate into methane and water. While the volume of water dissociated from hydrate is around 79% of the initial volume of hydrate, the volume of dissociated methane gas is dependent on pressure and temperature conditions. The modified Peng-Robinson equation of state (PRSV) is used to compute the volume of methane gas during depressurization [Stryjek and Vera, 1986]:

$$P_g = \frac{RT_g}{V_g - b} - \frac{a}{V_g(V_g + b) + b(V_g - b)} \quad (5)$$

where P_g is the gas pressure, T_g is the gas temperature, V_g is the volume of gas per mole of gas, R is the universal gas constant, and the values of a and b are parameters for methane gas which are tabulated in Jang and Santamarina (2011) as well as other parameters.

Differential pressure between gas and water in a tube of the pore network model is the capillary pressure that is a function of surface tension T_s , contact angle θ , and tube radius R_{tube} , $P_c = P_g - P_w = 2T_s \cos\theta / R_{\text{tube}}$ where the water-methane interfacial tension is $T_s = 0.072 \text{ mN/m}$ and the contact angle is assumed $\theta = 0^\circ$ for a perfectly wetting system.

Hydrate dissociation and gas expansion starts by gradually decreasing the water pressure at two opposite boundaries of the pore network model. Gas expands to the neighboring water pores if the gas pressure is higher than the summation of water pressure P_w and the capillary pressure P_c , $P_g > P_w + P_c$. Gas expands to water pores that have the minimum value of water pressure plus capillary pressure, $\min(P_w + P_c)$. Gas expands to the neighboring water clusters unless (1) gas pores surround an isolated water cluster (The isolated water cluster doesn't have an access to a water drainage path) or (2) the gas cluster does not satisfy the gas expansion condition, $P_g > P_w + P_c$. An extended Hoshen-Kopelman algorithm is used for clustering both water and gas pores during each step of depressurization [Hoshen and Kopelman, 1976; Al-Futaisi and Patzek, 2003].

Permeability calculation. At every gas expansion step, the pressure drop in the tubes of the pore network model is determined for both water and gas phase using Poiseuille equation, $\Delta P = 8\mu Q \Delta L / (\pi R_{\text{tube}}^4)$ where ΔP is the pressure drop, Q is the flow rate, ΔL is the length of tube, R_{tube} is the radius of tube, and μ is the dynamic viscosity of fluid (see Jang et al. 2011 for detailed procedure of hydraulic conductivity calculation).

4. Results

An initial hydrate saturation $S_h = 0.02$ is used for gas expansion simulation. For hydrate dissociation and gas expansion, the water pressure decreases from 13MPa to 0.1MPa at a given temperature 280K. The depressurization rate is assumed very slow so that the heat needed for hydrate dissociation is transported from the pore-network model boundaries to maintain constant temperature. Depressurization below hydrate stability boundary allows hydrates to dissociate into gas and gas expand (Figure 3a), and gas percolation occurs at the gas saturation $S_g = 0.12$ (Figure 3b). Gas expands more with further depressurization (Figure 3c). Gas continues to expand until the

water clusters lose a water drainage path. At every gas expansion step, water and gas conductivity is calculated and later divided by the reference conductivity of each phase.

Ten simulation runs are performed. For each simulation run, the location of hydrate pores is varied while initial hydrate saturation is maintained constant as $S_h=0.02$, and the configuration of the pore network model such as pore size, location and connectivity is also maintained constant. The water and gas relative permeability data of ten simulation runs are shown in Figure 4a.

As gas expands by displacing water, relative water permeability decreases. Relative gas permeability develops after gas percolation occurs at $S_g \approx 0.14$. The residual water saturation is $S_{rw} \approx 0.25$. The applied pressure drop (from 13MPa to 0.1MPa at 280K) results in ~ 170 times of volume expansion [Jang and Santamarina, 2011]. Therefore, theoretically, gas expansion from the initial hydrate saturation $S_h=0.02$ can displace all water initially existing in the pore-network model. The reason gas expansion stops is the loss of water drainage path. The residual water saturation of ten simulation runs is $S_{rw} \approx 0.26$, which is the saturation of water in isolated pores identified by the extended Hoshen-Kopelman algorithm.

5. Analyses and Discussion

The method of least squares is used to fit Equations 1~4 to relative water and gas permeability data of the pore-network model simulations. The water and gas permeability data of each simulation run is used to obtain the fitting parameters (Figure 4b). The fitting parameters, m for van Genuchten equation and n_w and n_g for modified Stone equation are obtained for ten simulation runs and summarized in Table 1.

For van Genuchten-type equations, the average of m -values (m_w) for relative water permeability is $\mu[m_w]=0.89$ with a standard deviation $\sigma[m_w]=0.03$, and the average of m -values (m_g) for relative gas permeability is $\mu[m_g]=0.68$ with a standard deviation $\sigma[m_g]=0.01$. These values are higher than the value $m \approx 0.45$ used in hydrate simulation studies in the literature.

For modified Stone-type equation, the average of n_w -values for relative water permeability is $\mu[n_w]=3.17$ with a standard deviation $\sigma[n_w]=0.22$, and the average of n_g -values for gas is $\mu[n_g]=1.31$ with a standard deviation $\sigma[n_g]=0.02$. The average of n_w -values ($\mu[n_w]=3.17$) is within the range of n_w -values used for hydrate simulation studies in the literature ($n_w=3.0 \sim 4.5$) while the averaged n_g -value ($\mu[n_g]=1.31$) is lower than the values used in the literature ($n_g=2.0 \sim 4.0$). These n_g -values used in the existing hydrate simulation studies may produce a gas permeability trend lower than that obtained in this paper.

Pore-network model simulation results show gas percolation starts at around $S_g \approx 0.14$ (Figure 4b) while the van Genuchten-type and modified Stone-type equations predict gas permeability develops at very low gas saturation near $S_g=0$ (Figure 4b).

This study assumes spatially randomly distributed hydrate pores. The hydrate morphology (distributed-vs.-patchy formation) and initial saturation affect physical properties of hydrate-bearing sediments such as electrical, hydraulic, and thermal conductivity and bulk modulus [Dai et al., 2012]. Therefore, the effects of hydrate morphology and saturation on relative permeability curves should be explored further.

Gas viscosity decreases with decreasing gas pressure at a given temperature. For example, methane viscosity varies from $\mu=20.2$ [$\mu\text{Pa}\cdot\text{s}$] at $P=20.5\text{MPa}$ to $\mu=11.6$ [$\mu\text{Pa}\cdot\text{s}$] at $P=3.2\text{MPa}$ under constant

temperature $T=298.15\text{K}$ [Van der Gulik et al., 1988]. However, this study does not consider pressure-dependent gas viscosity change. Gas saturation increases with continued gas expansion due to depressurization. Therefore, gas viscosity will decrease as gas saturation increases, which will affect gas permeability.

6. Conclusions

The selection of appropriate fitting parameters for relative permeability equations is very important to predict water and gas production from hydrate-bearing sediments. In this study, a pore-network model simulation is performed to suggest proper fitting parameters.

The results of a pore-network model simulation show that van Genuchten-type and modified Stone-type equations can be used to predict relative water and gas permeability for the gas production from hydrate-bearing sediments with properly chosen fitting parameters.

For van Genuchten-type equations, two fitting parameters are suggested for the relative permeability of water and gas phase: $m_w=0.89$ for water and $m_g=0.68$ for gas. These suggested fitting parameters are higher than the m -value $m\approx 0.45$ used in the literature for hydrate numerical simulation studies.

The suggested fitting parameters for modified Stone-type equations are $n_w=3.17$ and $n_g=1.31$. The fitting parameter for water permeability is within the range of n_w -values used for hydrate simulation studies in the literature ($n_w=3.0\sim 4.5$). However, the n_g -value is lower than the values used in the literature ($n_g=2.0\sim 4.0$).

Especially, both van Genuchten-type and modified Stone-type equations predict gas permeability develops even at low gas saturation near zero, but the numerical simulation results show that gas permeability develops after gas percolation occurs at $S_g\approx 0.14$.

Even though the effect of hydrate morphology, saturation, and gas viscosity on relative permeability need to be considered for more reliable study, this study is the first attempt to suggest fitting parameters of relative permeability equations for gas production from hydrate-bearing sediments.

References

- Al-Futaisi, A., and T. W. Patzek (2003), Extension of Hoshen-Kopelman algorithm to non-lattice environments, *Physica A*, 321, 665–678.
- Al-Kharusi, A.S. and Blunt, M.J. (2007), Network extraction from sandstone and carbonate pore space images, *Journal of Petroleum Science and Engineering*, 56, 219-231.
- Anderson, B.J., Kurihara, M., White, M.D., Moridis, G.J., Wilson, S.J., Pooladi-Darvish, M., Gaddipati, M., Masuda, Y., Collett, T.S., Hunter, R.B., Narita, H., Rose, K., Boswell, R. (2011), Regional long-term production modeling from a single well test, Mount Elbert gas hydrate stratigraphic test well, Alaska North slope, *Journal of Marine Petroleum Geology*, 28, 493-501.
- ASTM D6836, Standard test methods for determination of the soil water characteristic curve for desorption using hanging column, pressure extractor, chilled mirror hydrometer, or centrifuge.
- Brooks, R.H. and Corey, A.T. (1964), Hydraulic properties of porous medium, *Hydrology paper No.3*, Civil engineering department, Colorado state university, Fort Collins, Colorado.
- Corey, A.T. (1954), The interrelation between gas and oil relative permeabilities, *Producers monthly*, 19(1), 38-41.
- Dai, S. and Santamarina, J.C. (2013), Water retention curve for hydrate-bearing sediments, *Geophysical Research Letters*, 40, doi:10.1002/2013GL057884.

- Dai, S., Santamarina, J.C., Waite, W.F., and Kneafsey, T.J. (2012), Hydrate morphology: Physical properties of sands with patchy hydrate saturation, *Journal of Geophysical Research – Solid Earth*, 117, B11205.
- Dong, H. (2007), Micro-CT imaging and pore network extraction, PhD thesis, Imperial College London.
- Dong, H. and Blunt, M.J. (2009), Pore-network extraction from micro-computerized-tomography images, *Physical Review E*, 80, 036307.
- Fredlund, D.G. (2002), Use of the soil-water characteristic curve in the implementation of unsaturated soil mechanics, *Proceedings of third international conference on unsaturated soils*, Recife, Brazil, March, 887-902.
- Fredlund D.G. and Xing, A. (1994), Equations for the soil-water characteristic curve, *Canadian geotechnical journal*, 31, 521-532.
- Ginsburg, G., Soloviev, V., Matveeva, T., and Andreeva, I. (2000), Sediment grain-size control on gas hydrate presence, Sites 994, 995, and 997, Scientific Results, Proceedings of the Ocean Drilling Program, Scientific Results, 164, doi:10.2973/odp.proc.sr.164.236.2000.
- Gupta, A. (2007), Methane hydrate dissociation measurements and modeling: The role of heat transfer and reaction kinetics, *Ph.D. thesis*, Colorado School of Mines.
- Hong, H. and Pooladi-Darvish, M. (2003), A numerical study on gas production from formations containing gas hydrates, *Canadian international petroleum conference-54th Annual technical meeting*, June 10-12, Calgary, Canada.
- Hong, H. and Pooladi-Darvish, M. (2005a), Numerical study of constant-rate gas production from in situ gas hydrate by depressurization, in Scientific Results from the Mallik 2002 Gas Hydrate Production Research Well Program, Mackenzie Delta, Northwest Territories, Canada, ed.) Dallimore, S.R. and Collett, T.S., Geological Survey of Canada, Bulletin 585.
- Hong, H. and Pooladi-Darvish, M. (2005b), Simulation of depressurization for gas production from gas hydrate reservoirs, *Journal of Canadian Petroleum Technology*, 44(11), 39-46.
- Hoshen, J., and R. Kopelman (1976), Percolation and cluster distribution. I. Cluster multiple labeling technique and critical concentration algorithm, *Phys. Rev. B*, 14(8), 3438-3445.
- Jaiswal, N.J. (2004), *Measurement of gas-water relative permeabilities in hydrate systems*, MS thesis, University of Alaska, Fairbanks, Alaska.
- Jang, J. and Santamarina, J.C. (2011), Recoverable gas from hydrate-bearing sediments: Pore network model simulation and macroscale analyses, *Journal of Geophysical Research – Solid Earth*, 116, B08202.
- Jang, J. and Santamarina, J.C. (2014), Evolution of saturation and relative permeability during gas production from hydrate-bearing sediments – Gas invasion vs. Gas nucleation, *Journal of Geophysical Research – Solid Earth*, under review.
- Jang, J., Narsilio, G.A., and Santamarina, J.C. (2011), Hydraulic conductivity in spatially varying media – a pore-scale investigation, *Geophysical Journal International*, 184, 1167-1179.
- Jenner, K.A., Dallimore, S.R., Clark, I.D., and Medioli, B.E. (1999), Sedimentology of gas hydrate host strata from the JAPEx/JNOc/GSC Mallik 2L-38 gas hydrate research well, in *Scientific Results from JAPEx/JNOc/GSC Mallik 2L-38 Gas Hydrate Research Well, Mackenzie Delta, Northwest Territories, Canada* (ed.) S.R. Dallimore, T. Uchida and T.S. Collett; Geological Survey of Canada, Bulletin 544, 57-68.
- Johnson, A., Patil, S., and Dandekar, A. (2011), Experimental investigation of gas-water relative permeability for gas-hydrate-bearing sediments from the Mount Elbert gas hydrate stratigraphic test well, Alaska north slope, *Marine and petroleum geology*, 28, 419-426.
- Kleinberg, R.L., Flaum, C., Griffin, D.D., Brewer, P.G., Malby, G.E., Peltzer, E.T., and Yesinowski, J.P. (2003), Deep sea NMR: Methane hydrate growth habit in porous media and its relationship to hydraulic permeability, deposit accumulation, and submarine slope stability, *Journal of geophysical research*, 108(10), 2508.

- Konno, Y., Masuda, Y., Hariguchi, Y., Kurihara, M., and Ouchi, H. (2010), Key factors for depressurization-induced gas production from oceanic methane hydrates, *Energy&Fuels*, 24, 1736-1744.
- Kurihara, M., Funatsu, K., Ouchi, H., Masuda, Y., Yasuda, M., Yamamoto, K., Numasawa, M., Fujii, T., Narita, H., Dallimore, S.R., Wright, F. (2008), Analysis of the JOGMEC/NRCAN/Aurora Mallik gas hydrate production test through numerical simulation, Proceedings of 6th international conference on gas hydrates, Vancouver, British Columbia, Canada, July 6~10.
- Kurihara, M., Sato, A., Funatsu, K., Ouchi, H., Masuda, Y., Narita, H., and Collett, T.S. (2011), Analysis of formation pressure test results in the Mount Elbert methane hydrate reservoir through numerical simulation, *Marine and petroleum geology*, 28(2), 502-516.
- Minagawa, H., Hirakawa, Y., Sato, M., Ohmura, R., Kamata, Y., Takeya, S., Nagao, J., Ebinuma, T., Narita, H., and Masuda, Y. (2004), Measurement of water permeability under the presence of methane hydrate, *AAPG Hedberg research conference*, Vancouver, BC, Canada, Sep. 12-16.
- Minagawa, H., Nishikawa, Y., Ikeda, I., Sakamoto, Y., Komai, T., and Narita, H. (2007), Measurement of methane hydrate sediment permeability using several chemical solutions as inhibitors, *The seventh ISOPE ocean mining symposium*, Lisbon, Portugal, July 1-6.
- Moridis, G.J., and Kowalsky, M.B. (2005), Depressurization-induced gas production from class-1 hydrate deposits, *SPE Annual Technical Conference and Exhibition*, Dallas, TX, ISA, 9-12 Oct., SPE97266.
- Moridis, G.J. and Reagan, M.T. (2007a), Gas production from oceanic class 2 hydrate accumulations, *Offshore Technology Conference*, Houston, TX, USA.
- Moridis, G.J. and Reagan, M.T. (2007b), Strategies for gas production from oceanic class 3 hydrate accumulations, *Offshore Technology Conference*, OTC 18865, Houston, TX, USA.
- Moridis, G.J. and Sloan, E.D. (2007), Gas production potential of disperse low-saturation hydrate accumulations in oceanic sediments, *Energy conversion and management*, 48(6), 1834-1849.
- Moridis, G.J., Kowalsky, M., and Pruess, K. (2007), Depressurization-induced gas production from class1 hydrate deposits, *SPE Journal of Reservoir Evaluation & Engineering*, 10(5), 458-481.
- Moridis, G.J., Kowalsky, M.B., and Pruess, K. (2008), TOUGH+HYDRATE v1.0 user's manual: a code for the simulation of system behavior in hydrate-bearing geologic media, LBNL-149E.
- Moridis, G.J., Reagan, M.T., Kim, S.-J., Seol, Y., Zhang, K. (2009), Evaluation of the gas production potential of marine hydrate deposits in the Ulleung Basin of the Korea East Sea 2007 SPE Asia Pacific Oil&Gas Conference and Exhibition, Jakarta, Indonesia, Oct 30~Nov 1, SPE 110859.
- Myshakin, E.M., Anderson, B.J., Rose, K., Boswell, R., (2011), Simulations of variable bottomhole pressure regimes to improve production from the double-unit Mount Elbert, Milne Point Unit, North Slope Alaska hydrate deposit, *Energy & Fuels*, 25, 1077-1091.
- Myshakin, E.M., Gaddipati, M., Rose, K., and Anderson, B.J. (2012), Numerical simulations of depressurization-induced gas production from gas hydrate reservoirs at the Walker Ridge 313 site, northern Gulf of Mexico, *Marine and Petroleum Geology*, 34, 169-185.
- Parker, J.C., Lenhard, R.J., and Koppusamy, T. (1987), A parametric model for constitutive properties governing multiphase flow in porous media, *Water Resources Research*, 23, 618-624
- Phadnis, H.S. and Santamarina, J.C. (2011), Bacteria in sediments: pore size effects, *Géotechnique Letters*, 1, 91-93.
- Poulsen, S., McDougall, S.R., Sorbie, K., and Skauge, A. (2001), Network modeling of internal and external gas drive, *International symposium of the society of core analysts*, Edinburgh, Sep., SCA2001-17.
- Reagan, M.T. and Moridis, G.J. (2008), Dynamic response of oceanic hydrate deposits to ocean temperature change, *Journal of Geophysical Research*, 113, C12023.

- Reagan, M.T., Kowalsky, M.B., Moridis, G.J., and Silpngarmert, S. (2010), The effect of reservoir heterogeneity on gas production from hydrate accumulations in the permafrost, *SPE Western Regional Meeting*, Anaheim, CA, USA, 27-29 May.
- Rutqvist, J. and Moridis, G.J. (2007), Numerical studies of geomechanical stability of hydrate-bearing sediments, *Offshore Technology Conference*, Houston, TX, USA, Apr. 30- May 3.
- Rutqvist, J. and Moridis, G.J. (2009), Numerical studies on the geomechanical stability of hydrate-bearing sediments, *SPE Journal*, 14(2), 267-282.
- Silin, D.B. and Patzek, T.W. (2006), Pore space morphology analysis using maximal inscribed spheres, *Physica A*, 371, 336-360.
- Soga, K., Lee, S.L., Ng, M.Y.A., and Klar, A. (2007), Characterisation and engineering properties of methane hydrate soils, in *Characterisation and Engineering Properties of Natural Soils*, pp. 2591-2642, Taylor-Francis, London.
- Stone, H.L. (1970), Probability model for estimating three-phase relative permeability, *Journal of petroleum technology*, 214-218.
- Stryjek, R., and J. H. Vera (1986), PRSV: An improved Peng-Robinson equation of state for pure compounds and mixture, *Can. J. Chem. Eng.*, 64, 323-333.
- Tan, B.B. (2004), *Geotechnical characteristic of sediments from Hydrate Ridge, Cascadia continental margin*, MSc thesis, Massachusetts Institute of Technology, Dept. of Civil and Environmental Engineering.
- Uddin, M., Coombe, D., Law, D., and Gunter, B. (2008), Numerical studies of gas hydrate formation and decomposition in a geological reservoir, *Journal of energy resources technology*, 130, 032501.
- Van der Gulik, P.S., Mostert, R., and Van den Berg (1988), The viscosity of methane at 25C up to 10kbar, *Physica A*, 151, 153-166.
- van Genuchten, M.Th. (1980), A closed-form equation for predicting the hydraulic conductivity of unsaturated soils, *Soil Science Society of America Journal*, 44, 892-898.
- Wösten, J.H.M., Lilly, A., Nemes, A., and Bas, C.L. (1999), Development and use of a database of hydraulic properties of European soils, *Geoderma*, 90, 169-185.
- Yortsos, Y.C. and Parlar, M. (1989). Phase change in binary systems in porous media: Application to solution-gas drive, *SPE annual technical conference and exhibition*, SPE 19697, 693-708.

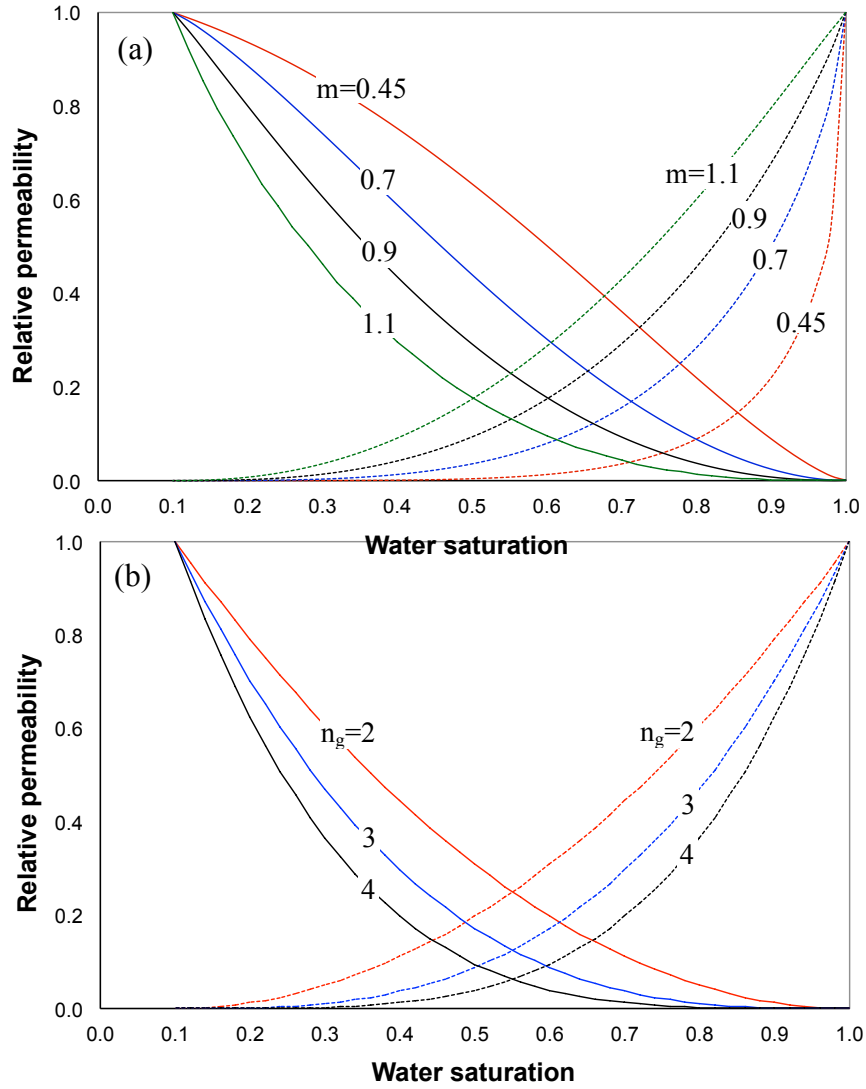


Figure 1. Relative water and gas permeability curves of van Genuchten-type and modified Stone-type equations with several fitting parameters. (a) Relative permeability curves of van Genuchten-type. Used m -values are $m=0.45, 0.7, 0.9,$ and 1.0 . (b) Relative permeability curves of modified Stone-type. Used n_w - and n_g -values are $n_w=n_g=2.5, 3, 3.5,$ and 4 .

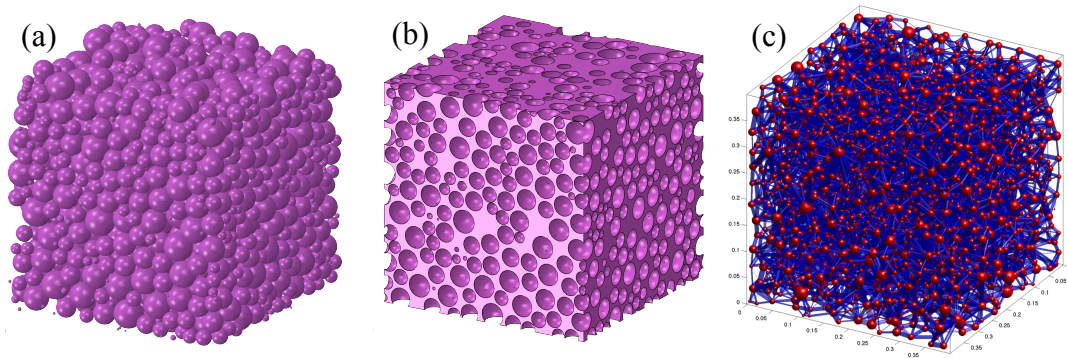


Figure 2. Sequence of pore-network model generation. (a) Particle packing generated by discrete element model. The maximum particle diameter is $D_{\max}=0.52\text{mm}$, the minimum particle diameter is $D_{\min}=0.04\text{mm}$, the coefficient of uniformity is $c_u=D_{60}/D_{10}=0.3\text{mm}/0.09\text{mm}=3.3$, and the coefficient of curvature is $c_c=D_{60}^2/(D_{10}D_{30})=(0.3\text{mm})^2/(0.09\text{mm}\times 0.21\text{mm})=4.8$ (Here, D_X is the particle diameter representing that $X\%$ of total particles is smaller than D_X). The dimension of the selected packing is $4\text{mm}\times 4\text{mm}\times 4\text{mm}$. The packing consists of 2183 particles. (b) Pore space of the particle packing. (c) Extracted pore network. The extracted pore network model consists of 2,921 pores and 12,260 tubes with the tube connectivity at pore (coordination number) of $cn=4.2$. Mean pore radius is $\mu[R_{\text{pore}}]=54\mu\text{m}$ and standard deviation in pore radius in logarithmic scale is $\sigma[\ln(R_{\text{pore}})]=0.42$, which is within the range of standard deviation in pore size of natural sediments obtained by mercury intrusion porosimetry $\sigma[\ln(R_{\text{pore}})]=0.4\pm 0.2$ [Phadnis and Santamarina, 2011]. Mean tube radius is $\mu[R_{\text{tube}}]=24\mu\text{m}$.

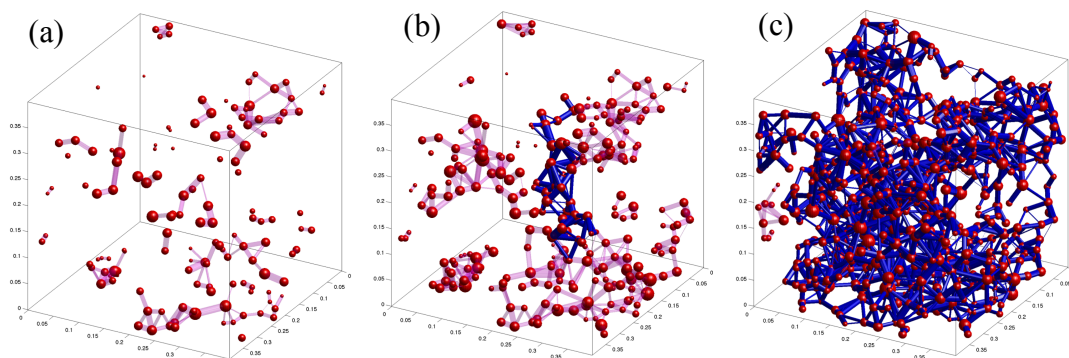


Figure 3. Gas expansion by depressurization: (a) Gas expansion after hydrate dissociation at $S_g=0.05$. (b) Gas percolation occurred at $S_g=0.12$. (c) Gas expansion at $S_g=0.3$. Note that only gas pores are shown as red color. Tubes in isolated gas clusters are colored as light red, and tubes in percolated gas clusters are colored as blue.

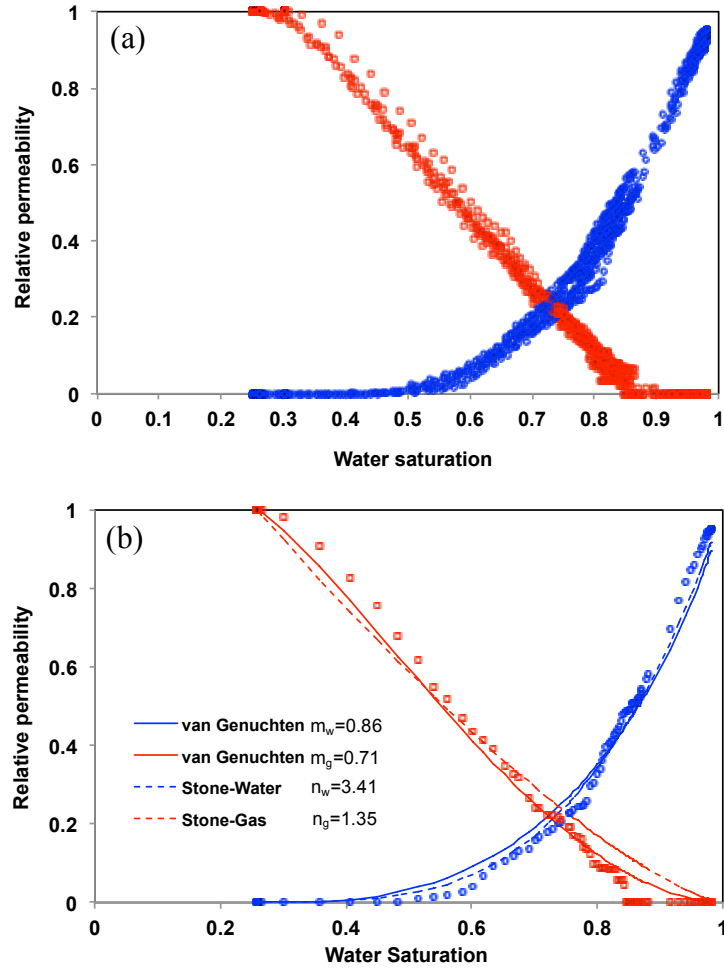


Figure 4. Relative water and gas permeability simulation results and fitted curves. (a) Relative water and gas permeability data of 10 simulation runs. (b) van Genuchten- and modified Stone-type curves fitted to numerical simulation results (Simulation #1). The fitting parameters are obtained by using the method of least squares. Note that especially for modified Stone-type equations, the residual gas saturation is assumed to be zero $S_{rg}=0$ so that the relative gas permeability k_{rw} changes from 1 to 0 (Equation 4).

Table 1. Fitting parameters of van Genuchten-type and modified Stone-type equations obtained from 10 simulation runs.

Simulation Runs	van Genuchten		modified Stone		Residual water saturation S_{rw}	Gas saturation S_g at percolation
	m_w	m_g	n_w	n_g		
1	0.86	0.71	3.41	1.35	0.26	0.16
2	0.92	0.68	3.03	1.35	0.25	0.14
3	0.88	0.69	3.24	1.31	0.25	0.13
4	0.85	0.66	3.28	1.29	0.25	0.12
5	0.86	0.69	3.50	1.33	0.25	0.10
6	0.88	0.67	3.28	1.29	0.26	0.11
7	0.88	0.66	3.26	1.29	0.26	0.14
8	0.93	0.68	2.94	1.31	0.26	0.14
9	0.93	0.68	2.93	1.32	0.26	0.15
10	0.94	0.66	2.85	1.31	0.30	0.19
Average	0.89	0.68	3.17	1.31	0.26	0.14
St. Dev.	0.03	0.01	0.22	0.02	0.01	0.03

National Energy Technology Laboratory

626 Cochrans Mill Road
P.O. Box 10940
Pittsburgh, PA 15236-0940

3610 Collins Ferry Road
P.O. Box 880
Morgantown, WV 26507-0880

13131 Dairy Ashford Road, Suite 225
Sugar Land, TX 77478

1450 Queen Avenue SW
Albany, OR 97321-2198

Arctic Energy Office
420 L Street, Suite 305
Anchorage, AK 99501

Visit the NETL website at:
www.netl.doe.gov

Customer Service Line:
1-800-553-7681

